

Supplementary Material for “A Ferromagnetic Skyrmion-Based Diode with Voltage-Controlled Potential Barrier”

Li Zhao,^a Xue Liang,^a Jing Xia,^b Guoping Zhao,^{a,c,d,*} and Yan Zhou^b

^a *College of Physics and Electronic Engineering, Sichuan Normal University, Chengdu 610068, China*

^b *School of Science and Engineering, The Chinese University of Hong Kong, Shenzhen, Guangdong 518172, China*

^c *State Key Laboratory of Metastable Materials Science and Technology, Yanshan University, Qinhuangdao 066004, China*

^d *Collaborative Innovation Center for Shanxi Advanced Permanent Materials and Technology, Linfen 041004, China*

*Email: zhaogp@uestc.edu.cn

Supplementary Note 1. The influence of the parameters on the saturation velocity v_s of the skyrmion

In the main text, it is found that as the ratio m of PMA between the boundary and middle on the nanotrack increases, $m = K_b / K_m$, the maximum velocity v_x of the skyrmion tends to a saturation value when the driving current density j is constant. Here, we discuss the influence of parameters from Table 1 on the saturation velocity v_s at different high-anisotropy boundary width w_0 , as shown in Fig. S1. With the enlargement of exchange stiffness A or anisotropy constant K , the velocity v_s goes down, as expressed in Fig. S1(b) or Fig. S1(c). It is well known that the larger the two material parameters are, the more difficult it is for the polarization current to flip the magnetic moment, resulting in the decrease of the skyrmion velocity. However, the velocity v_s goes up when DMI constant D rises shown in Fig. S1(d). DMI leads adjacent magnetic moments to align vertically, which is conducive to the deflection of magnetic moments. Besides, the damping coefficient α is almost inversely proportional to the velocity v_s , while the polarizability rate P is basically proportional to it, which all conform to Eq. (4) in the next paragraph. Interestingly, the velocity v_s does not decrease with the increase of saturation magnetization M_s as the equation shows, but decreases first and then builds up. Because when M_s is large, the effect of demagnetization energy cannot be ignored, resulting in the decrease of effective K_{eff} , $K_{eff} = K - \frac{1}{2}u_0M_s^2$. Moreover, it can be seen that the velocity v_s is independent of high-anisotropy boundary width w_0 .

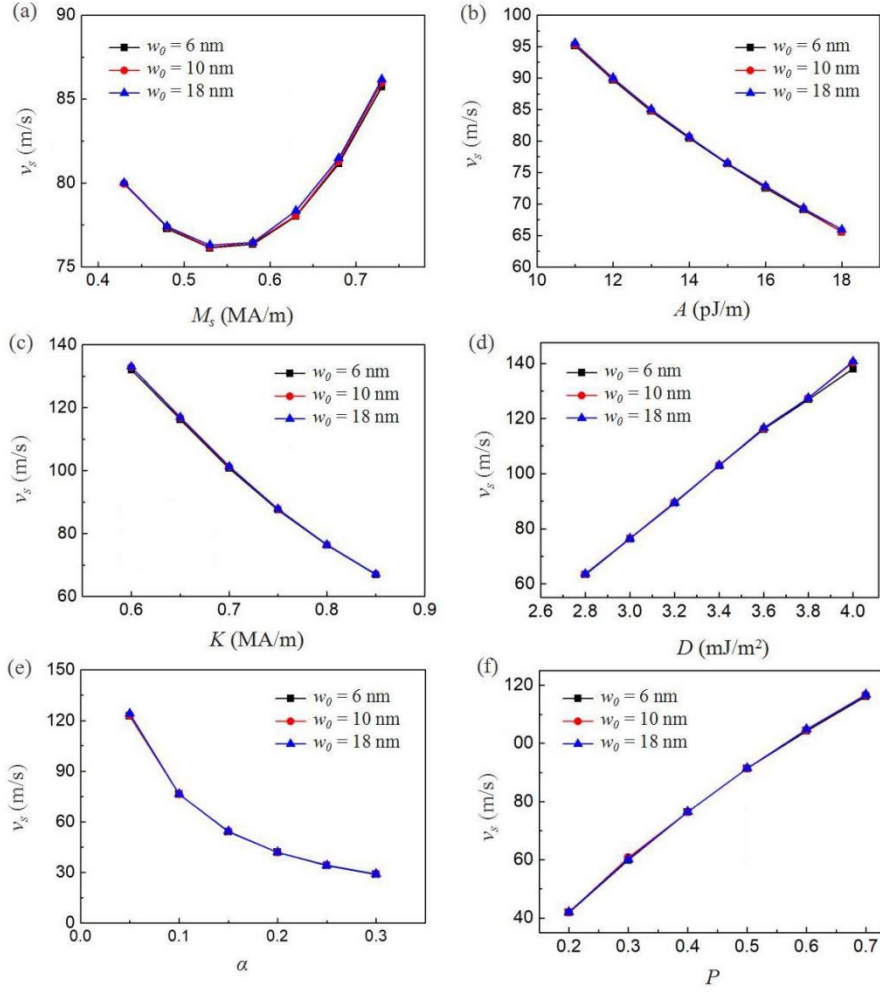


Fig. S1 the saturation velocity v_s of the skyrmion in the x -axis as functions of (a) saturation magnetization M_s , (b) exchange stiffness A , (c) anisotropy constant K , (d) DMI constant D , (e) damping coefficient α and (f) polarizability rate P . The skyrmion is driven by the driving current j of 2 MA/cm² on the nanotrack in scheme A. And there is a trapezoid with the lower left corner φ of 45°, length l of 300 nm and width w of 30 nm on the nanotrack with different high-anisotropy boundary width $w_0 = 10$ nm.

When the skyrmion moves on a restricted nanotrack, the force F generated by the potential energy of the surrounding environment should be taken into account. For CPP, Thiele equation is written as

$$\mathbf{G} \times \mathbf{v} + \alpha \mathbf{D} \cdot \mathbf{v} - b \mathbf{R} \cdot \mathbf{j}_{HM} + \mathbf{f} = 0 \quad (1)$$

Here, the vector $\overset{\mathbf{t}}{G}$ can be identified as the gyrocoupling vector, $\overset{\mathbf{t}}{G} = (0, 0, 4\pi Q)$. $\overset{\mathbf{t}}{v}$ is the velocity of the skyrmion. The coefficient α is the Gilbert damping. And the matrix $\overset{\mathbf{t}}{D} = \begin{pmatrix} D & 0 \\ 0 & D \end{pmatrix}$ is the dissipative tensor, $D = \int \partial_x \overset{\mathbf{r}}{m} \cdot \partial_x \overset{\mathbf{r}}{m} dx dy$. Where $b = \frac{\hbar j P \gamma}{2u_0 e M_s t_F}$, with the simulation film thickness t_F , the reduced Plank constant \hbar , the applied current density j , the spin polarization rate P and the elementary charge e , the saturation magnetization M_s , γ is the Landau-Lifshitz gyromagnetic ratio. $\overset{\mathbf{t}}{R}$ is the in-plane rotation matrix, which is related to the configuration of the skyrmion. For the Neel skyrmion, $\overset{\mathbf{t}}{R} = \begin{pmatrix} R & 0 \\ 0 & R \end{pmatrix}$, $R = \int (\overset{\mathbf{t}}{P} \times \overset{\mathbf{r}}{m}) \cdot \partial_x \overset{\mathbf{r}}{m} dx dy$. And $\overset{\mathbf{t}}{P}$ is the spin polarization direction, $\overset{\mathbf{t}}{P} = -e_y$. $\overset{\mathbf{t}}{j}_{HM}$ represents the direction of the current passing through the heavy metal layer, which is along the $+x$ axis in the simulation. In addition, $\overset{\mathbf{t}}{f}$ has to do with the potential energy of the boundary on the nanotrack. Due to the forward moving skyrmion is close to the upper boundary during the motion, we mainly consider the repulsive force along the y axis from the upper boundary here, $\overset{\mathbf{t}}{f} = -f_y e_y$.

The steady velocity formula of a ferromagnetic skyrmion can be obtained by solving the Thiele equation, written as

$$v_x = \frac{\alpha D b R + G f_y}{G^2 + \alpha^2 D^2} \quad (2a)$$

$$v_y = \frac{-G b R + \alpha D f_y}{G^2 + \alpha^2 D^2} \quad (2b)$$

Suppose the repulsion force of the boundary is large enough to completely overcome SkHE,

$$v_x = \frac{b R}{\alpha D} \quad (3a)$$

$$v_y = 0. \quad (3b)$$

In the simulation for the saturation velocity v_s of the skyrmion, we find that the velocity along the y direction is very close to 0 when the motion of the skyrmion is stable. It shows that SkHE is basically overcome by the high-anisotropy boundary, and the saturation velocity v_s can be written as

$$v_s = \frac{bR}{\alpha D}. \quad (4)$$

Supplementary Note 2. The relationship between the driving current density and one-way motion of skyrmion

In addition to the geometric parameters of the trapezoid region and the PMA K_b at the boundary (including the trapezoid part), the driving current density j also affects the one-way motion of the skyrmion. Fig. S2 are phase diagrams for one-way motion of the skyrmion with various ratio m , trapezoidal lower left corner φ , trapezoid width w , trapezoid length l and driving current density j . The m is the ratio of PMA between the boundary (including the trapezoid part) and middle of the nanotrack in scheme A, $m = K_b / K_m$. From Fig. S2(a), it is obvious that the higher the PMA in the high-anisotropy region, the greater the driving current for the skyrmion-based diode to work normally. Besides, the driving current density for one-way motion of the skyrmion can be appropriately adjusted by the trapezoidal length l . However, compared to the PMA in the high-anisotropy region and the trapezoidal length l , the trapezoidal width w and lower left corner φ have little effects on the driving current density, as shown in Fig. S2(b-c). Furthermore, when the driving current density is high, the skyrmion in forward motion is annihilated near the upper boundary due to SkHE. But the skyrmion in reverse motion enters the trapezoid region and then annihilates near the lower boundary of the nanotrack. When the current density continues to go up, the skyrmion in reverse motion annihilates directly and does not enter the trapezoidal region.

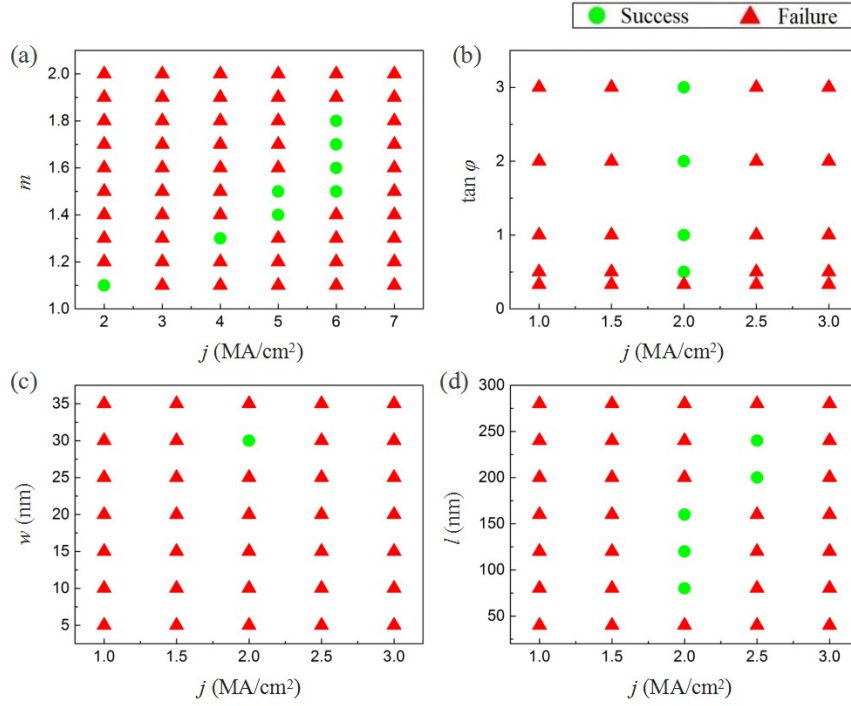


Fig. S2 Phase diagrams for one-way motion of the skyrmion with different (a) ratio m , (b) trapezoidal lower left corner ϕ , (c) trapezoid width w , (d) trapezoid length l and driving current j . The m is the ratio of PMA between the boundary (including the trapezoid part) and middle of the nanotrack. The skyrmion moves on the nanotrack with the high-anisotropy boundary width w_0 of 10 nm in scheme A. For (a), $w = 30$ nm, $l = 100$ nm, $\phi = 45^\circ$ ($\tan\phi = 1$). In (b), $w = 30$ nm, $l = 100$ nm, $m = 1.1$. For (c), $l = 100$ nm, $\phi = 45^\circ$ ($\tan\phi = 1$), $m = 1.1$. In (d), $w = 30$ nm, $\phi = 45^\circ$ ($\tan\phi = 1$), $m = 1.1$. The filled red triangle and the green circle stands for the failure and success of one-way motion of the skyrmion, respectively.

Supplementary Note 3. The robustness for one-way motion of the skyrmion over the variation of the parameters

Fig. S3 shows the realization for one-way motion of the skyrmion at different parameters. In the simulation, we randomly selected three groups of the trapezoidal length l and width w from the green part of Fig. 4(d) in the main text. For $w = 28$ nm and $l = 200$ nm, when the saturation magnetization M_s , exchange stiffness A , anisotropy constant K , DMI constant D and damping coefficient α vary by about 17.2%, 26.7%, 12.5%, 6.7%, 20% respectively, the one-way motion of the skyrmion can still be realized. But when the increase of polarizability rate P is more than 12.5%, the one-way motion of the skyrmion fails. Moreover, the calculation results of the other two groups of trapezoidal length l and width w does not differ significantly. Compared with other parameters, D is less robust for the results due to the influence on the size and formation of the skyrmion. The skyrmion cannot exist stably with small D (in this simulation, $D \leq 2.5$ mJ/m²), while it also obviously gets bigger as D goes up, which is easy to be clogged by the high-anisotropy trapezoidal region. To sum up, it can be seen from Fig. S3 that the one-way motion of the skyrmion have certain robust on the variation of the parameters in Table 1, which proves that the design has certain feasibility in experiments.

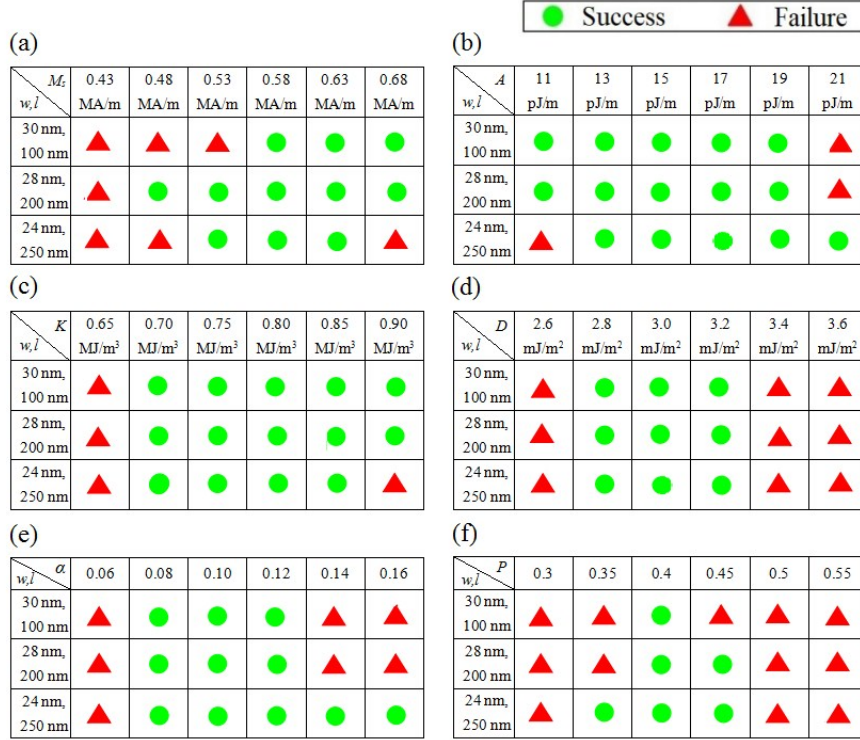


Fig. S3 The implementation for one-way motion of the skyrmion with various (a) saturation magnetization M_s , (b) exchange stiffness A , (c) anisotropy constant K , (d) DMI constant D , (e) damping coefficient α and (f) polarizability rate P . The skyrmion is driven by the driving current j of 2 MA/cm² on the nanotrack in scheme A. In the simulation, three groups of the trapezoidal length l and width w are calculated, which are 30 nm and 100 nm, 28 nm and 200 nm, 24 nm and 250 nm, respectively. A trapezoid with the lower left corner φ of 45° is located on the nanotrack, whose high-anisotropy boundary width w_0 is 10 nm. And the ratio m of PMA between the boundary (including the trapezoid part) and middle of the nanotrack is 1.1, $m = K_b / K_m$. The failure and success for one-way motion of the skyrmion is represented by the filled red triangle and the green circle, respectively.

Supplementary Note 4. The effect of voltage-induced variation of DMI on the motion of skyrmion.

Here, the effect of the applied voltage on the motion of the skyrmion is mainly discussed. The ratio of PMA and DMI constant between the boundary (including the trapezoid part) and middle of the nanotrack is represented by m and i respectively, $m = K_b / K_m$, $i = D_b / D_m$. When the change of PMA is larger than that of DMI, the skyrmion can move smoothly to the end of the nanotrack, as shown in Fig. S4(a). It means the large-DMI boundary is not conducive to the suppression of SkHE on the nanotrack. Recently, the experiment of Aik Jun Tan *et al.* demonstrated that a greater reversible conversion of PMA can be obtained by H⁺ pumping with the small gate voltage at room temperature, and the VCMA efficiency can be up to 5000 fJ/Vm^[1]. So we principally simulate the case where m is large in the research for the motion of the skyrmion. It can be seen from the Fig. S4(b) that the large-DMI boundary can also improve the maximum velocity v_x of the skyrmion along the nanotrack, which is weaker than the high-anisotropy boundary. Moreover, the velocity v_x of the skyrmion goes down obviously when it is close to the large-DMI boundary. As soon as the skyrmion enters the large-DMI boundary, its spin configuration is quickly destroyed and then disappears.

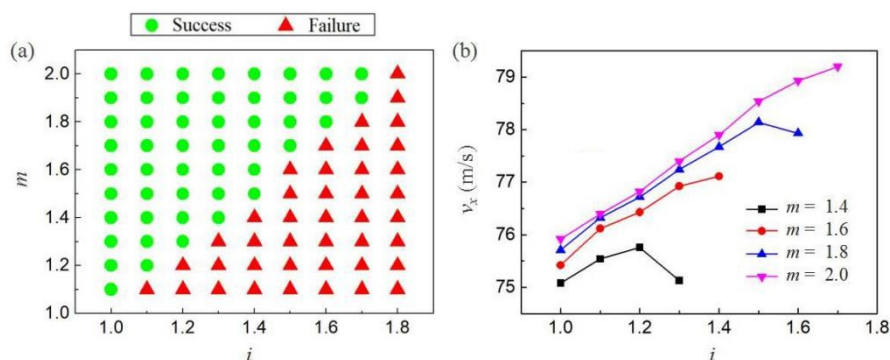


Fig. S4 (a) Phase diagram for the motion of the skyrmion with different ratio m and i . The m and i are the ratio of PMA and DMI constant between the boundary (including

the trapezoid part) and middle of the nanotrack respectively, $m = K_b / K_m$, $i = D_b / D_m$. And the filled red triangle indicates that the skyrmion fails to reach the end of the nanotrack, while the filled green circle indicates the success of the situation. (b) Relations between the maximum velocity v_x and the ratio i relation at the various ratio m . In the simulation, the skyrmion is driven by the driving current j of 2 MA/cm² on the nanotrack with the high-anisotropy boundary width w_0 of 10 nm in scheme A.

Supplementary References

1. A. J. Tan, M. Huang, C. O. Avci, F. Büttner, M. Mann, W. Hu, C. Mazzoli, S. Wilkins, H. L. Tuller and G. S. D. Beach, *Nature Materials*, 2018, **18**, 35-41.